Emergence of triplet correlations in superconductor/half-metallic nanojunctions with spin-active interfaces

Klaus Halterman*
Research and Intelligence Department, Physics Division, Naval Air Warfare Center, China Lake, California 93555, USA

Oriol T. Valls†
School of Physics and Astronomy, University of Minnesota, Minneapolis, Minnesota 55455, USA

(Received 7 July 2009; revised manuscript received 12 August 2009; published 8 September 2009)

We study triplet pairing correlations induced in an SFS trilayer (where F is a ferromagnet and S an ordinary *s*-wave superconductor) by spin-flip scattering at the interfaces, via the derivation and self-consistent solution of the appropriate Bogoliubov–de Gennes equations in the clean limit. We find that the spin-flip scattering generates $m=\pm 1$ triplet correlations, odd in time and study the general spatial behavior of these and of $m=0$ correlations as a function of position and of spin-flip strength, H_{spin}, concentrating on the case where the ferromagnet is half-metallic. For certain values of H_{spin}, the triplet correlations pervade the magnetic layer and can penetrate deeply into the superconductor. The behavior we find depends very strongly on whether the singlet order parameter is in the 0 or π state, which must in turn be determined self-consistently. We also present results for the density of states (DOS) and for the local magnetization, which, due to spin-flip processes, is not in general aligned with the magnetization of the half-metal, and near the interfaces, rotates as a function of position and H_{spin}. The average DOS in both F and S is shown to exhibit various subgap bound states positioned at energies that depend strongly on the particular junction state and the spin-flip scattering strength.

DOI: 10.1103/PhysRevB.80.104502 PACS number(s): 74.45.+c, 74.78.Fk, 74.78.Na

I. INTRODUCTION

Nanoscale structures involving ferromagnet (F) and superconductor (S) junctions illustrate the unique interaction of superconducting and ferromagnetic symmetries and provide a novel opportunity to study the powerful influence that the spin degree of freedom plays in transport and thermodynamic properties of such systems. The now well established variety of phenomena[1] induced by the resulting proximity effects, includes exotic singlet superconducting correlations, in particular the damped oscillatory Cooper pair amplitude in the magnet, with a spatial decay length in the clean limit over a few nanometers for strong magnets (such as Ni, Co, and Fe), and considerably less than the superconductor coherence length ξ_0. These oscillations lead to the possibility of switching between 0 and π junction states, with considerable potential[2] for applications. The superconductor region correspondingly becomes affected as it experiences the pair-breaking effects of the ferromagnet and becomes locally magnetized. These mutual effects depend considerably on the strength of the magnet and transparency of the interfaces, usually assumed spin-independent. If the interface scattering is generalized to include spin dependence, where the spin of the impinging electron is flipped when traversing the corresponding interface, the whole picture can be modified, including the emergence or enhancement of exotic triplet states, which involve odd frequency or different-time triplet correlations.

Triplet pairing correlations can arise in ferromagnet and superconductor heterostructures involving superconductors with a rotationally symmetric pairing symmetry (*s*-wave pairing), since they involve odd time symmetry pairing, as originally proposed[3] in a different context. In F-S structures the proximity effects associated with the magnet break spin rotation invariance. The superconducting order parameter in this scenario changes sign under time coordinate interchange of the two electrons comprising Cooper pairs. When a single quantization axis exists for the system, the only possible triplet pairing state is the one comprised of opposite spin pairs (the $m=0$ projection on the given quantization axis). If there exists noncollinear or inhomogeneous magnetization in the system, as can occur in structures involving differently oriented F layers or an in-plane spin-flip scattering potential, equal-spin $m=\pm 1$ triplet correlations can also arise. Several investigations into triplet effects in superconductor and ferromagnet hybrids has revealed a host of interesting and exotic phenomena,[4–6] including the possibility of a long-ranged superconductivity proximity effect in F-S structures. A new superconducting state that can potentially extend superconducting correlations into the magnetic region over long distances brings with it a host of useful device applications involving low temperature nanodevices, including nanoelectromechanical systems (NEMS), and superconducting circuits (π junctions with $I_0<0$).

While there has been recently considerable interest in trying to isolate and detect the triplet pairing state that is predicted to exist in such S-F structures, it can be difficult to disentangle the triplet and singlet correlations. It is therefore of interest to investigate heterostructures that restrict the singlet order parameter somewhat, yet retain the desired triplet correlations. The pinpointing of triplet effects can be exploited with the use of highly polarized materials, namely, half-metallic ferromagnets, where only a single spin channel is present at the Fermi level. The ordinary singlet pair amplitude is thus suppressed, since the magnet behaves essentially as an insulator for the opposite spin band. Several half-

metallic candidates are considered in connection with superconducting hybrids and spintronic applications. These include the conducting ferromagnet[6] CrO_2, the manganese perovskite[7,8] $La_{2/3}Ca_{1/3}MnO_3$, and the Heusler alloys,[9] possibly Co_2FeSi and Co_2MnSi, which are attractive from a nanofabrication standpoint, since growth by sputtering techniques is applicable. This is pertinent since CrO_2 cannot be grown by sputtering and is metastable. Thus it is of interest to determine the circumstances under which triplet correlations and related single-particle signatures emerge when a wide variety of spin flipping strengths for a half-metallic ferromagnet in F-S nanojunctions, with S being a conventional *s*-wave superconductor and interfacial spin-flip scattering providing the required symmetry breaking.

The spin-flip processes and their participation in proximity effects have been explored in several different experimental setups[6,10–12] possible in many instances due to advanced e-beam lithography and sputtering techniques. There is no current experiment however, that offers completely indisputable evidence of triplet correlations in ferromagnet and conventional superconductor hybrids, and thus further experimental investigations are needed. The spin flipping associated with the intrinsic exchange field in the ferromagnet in S-F bilayers was linked to critical temperature variations[10] as a function of F layer thicknesses. It was suggested that the measured Josephson current[6] in a sample with two NbTiN (*s*-wave) superconductors coupled by half-metallic CrO_2 is due to a supercurrent carried by spin triplet pairs since the electronic transport in CrO_2 is metallic solely for the spin-up band, and the expected magnet thickness for that system exceeded the estimated singlet correlation length for that sample. Current-voltage measurements,[11] in singlet superconductor-half-metallic point contacts revealed a marked resistance decrease and increased normal state conductance at small voltages, attributed to spin singlet-triplet conversion. Single particle spectroscopy results for the density of states (DOS) were also reported[12] for F-S bilayers including the strong ferromagnet, Ni. In that experiment, the conductance signature was measured as a function of ferromagnet thickness, d_F, revealing an interesting double peak structure and other subgap features that could not be theoretically accounted for within the dirty limit framework.

Numerous theoretical approaches involving spin-dependent scattering of some sort have helped pave the way toward unveiling the role of triplet pairing correlations in diffusive SFS hybrid nanostructures or clean[13] SFS junctions, both within the quasiclassical regime. The intermediate regime, separating diffusive and ballistic motion was also studied quasiclassically.[14,15] Any purely microscopic approaches, that retain quasiparticle information at the atomic scale, typically involved spin-independent scattering potentials at the interfaces.[16,17] If the pair-breaking mechanism of spin-flip scattering at the interfaces is included, the resultant interchange of spins yields complicated normal and Andreev reflection events. The investigation into these issues has been predominately in the diffusive regime however. Also, with relatively thick half-metals, self-consistent ballistic calculations[13] reveal that Josephson coupling can occur via triplet correlations from the singlet superconductor and spin mixing occurring at a spin-active interface. For calculations neglecting the mutual influence of superconducting and ferromagnet order parameters, spin-flip scattering was shown to also have a detrimental effect on the residual supercurrent, thus limiting such junctions as useful spin switches.[18] A long-range triplet component can arise[19] when the ferromagnet has a Néel domain structure where the in-plane magnetization rotates with changing depth in the magnet. The odd-frequency pairs arising from spin flipping at the junction interfaces can cause a peak in the local DOS of a diffusive half-metallic ferromagnet.[20] If the ferromagnet can be modeled by a conical magnetic structure,[21] as in Holmium, it was found that both singlet and triplet correlations undergo short range decay. Also, the decay length of the Josephson current was shown to decrease[22] with spin-flip and spin-orbit scattering, with spin-orbit scattering typically being the more destructive of the two. By illuminating the junction with microwave radiation at the proper resonance frequency however, the critical current can be enhanced,[23] due in part to singlet-triplet conversion processes. Nearly all of the cases studied thus far involve the quasiclassical method, and it is unclear how this landscape is modified when atomic length scales are not eliminated in the pertinent equations and when self-consistency of the singlet order parameter is taken into account.

In this paper, we address some of the above issues by presenting a fully self-consistent framework for a clean nanoscale trilayer junction comprised of a half-metal sandwiched between two conventional, *s*-wave superconductors. The pair-breaking mechanism is spin-flip scattering at the interfaces, which produces $m=\pm 1$ odd time pairs, and modifies the triplet $m=0$ component. The presence of two S layers, coupled through F via the proximity effect allows us to compare and contrast the 0 and π states. Our method is based on the quantum mechanical Bogoliubov–de Gennes (BdG) equations in the clean limit, which is ideal for half-metallic ferromagnets and proximity effects that can involve singlet correlations in the magnet with very short decay lengths of just a few nanometers. We are able to fully take into account proximity effects in the magnet and "inverse proximity effects" that arise in the superconductor regions, including the presence of a magnetic moment component normal to the magnetization in F. We employ a recently developed[24] method to determine the triplet correlations in such structures using a Heisenberg representation to derive the time-dependent quasiparticle wave functions. We consider spin-active interfaces by incorporating in-plane spin-dependent scattering in the effective Hamiltonian. By varying the spin scattering strength parameter, H_{spin}, over a broad range, long-range triplet correlations are shown to emerge and evolve. We study the spatial profile of all possible triplet correlations which depends on their corresponding projection onto the axis of quantization, which is taken to be along the fixed direction of magnetization in the half-metal (the z axis in our case). The relative admixtures of triplet amplitudes with total spin projection $m=0$ on the z axis (labeled f_0) and those with $m=1$ total spin projection quantum number, f_1, depend crucially on whether the junction is in a 0 or π state. The junction state with the lowest free energy, and its corresponding stability, is dictated not only by the geometry and spin splitting strength of the magnet,[25] but also by the mag-

nitude of spin scattering at the interfaces. An accurate determination of this requires a self-consistent calculation: this is even more evident when one considers that the triplet correlations in general peak near the interfaces, where self-consistency is most critical. After presenting the triplet correlations within the system as a function of the spin scattering strength, we turn our attention to the effect spin-active interfaces have on other physically important single-particle quantities such as the average DOS, and local magnetic moment. We find that the DOS has a subgap signature that depends on whether the junction is in a 0 or π state and the degree of spin scattering at the interfaces.

The rest of this paper is organized as follows: in Sec. II we discuss the methods we use to evaluate the order parameter in a fully self-consistent way and to determine the triplet correlations. We find, as in Ref. 17, that self-consistency is absolutely essential in order to correctly obtain the odd parity triplet correlations: without self-consistency, our numerical implementation of the quasiparticle expansions may yield nonvanishing equal-time triplet correlations near the interfaces, thus violating the Pauli principle. We review and discuss the appropriate quasiparticle expansions, the evaluation of the matrix elements, and other relevant details in the solution of the corresponding eigenvalue problem. The definition of the time-dependent triplet amplitudes is given and other quantities that are also of interest, such as the local magnetic moment and the local DOS are defined. Then, in Sec. III, the condensation energy, which reveals the relative stability of the 0 and π phases, is calculated as a function of H_{spin}. We then discuss in detail our results for the spatial and time behavior of the triplet amplitudes as a function of the spin-flip scattering strength. The associated penetration depths of the equal-spin triplet amplitudes into the superconductor reveal the long range nature of these correlations. Next, we focus on the averaged DOS in each region of competing order parameter symmetries, and display the spatial dependence of the local magnetic moment, as it relates to the inverse proximity effect. We show that the induced magnetic moment vector rotates near the interfaces. Finally, we give a summary of our results in Sec. IV.

II. METHODS

The SFS junction that we study is a trilayer structure infinite in the plane parallel to the interfaces, which we label the x-z plane, and with total length d in the y direction, normal to the interfaces. The width of each of the two superconductor layers is labeled by d_S and that of the ferromagnet by d_F. The superconductors are s-wave and identical. The entire structure occupies the space $0 \le y \le d$, with one superconductor occupying, $0 \le y \le d_S$, the ferromagnet: $d_S \le y \le d_S + d_F$, and the other superconductor, $d_S + d_F < y \le d$. There is spin-flip scattering at the interfaces, which will be described below.

To determine the equations governing triplet effects in SFS nanojunctions, we start with a fundamental quantity, the effective Hamiltonian, $\mathcal{H}_{\text{eff}}$, written in terms of creation and annihilation field operators and vector Pauli spin matrices, $\boldsymbol{\sigma}$,

$$\mathcal{H}_{\text{eff}} = \int d^3r \Bigg\{ \sum_{\alpha} \psi_{\alpha}^{\dagger}(\mathbf{r}) \left[-\frac{\boldsymbol{\nabla}^2}{2m} - E_F + V_0(\mathbf{r}) \right] \psi_{\alpha}(\mathbf{r}) + \sum_{\alpha,\beta} \psi_{\alpha}^{\dagger}(\mathbf{r}) (\mathbf{V} \cdot \boldsymbol{\sigma})_{\alpha\beta} \psi_{\beta}(\mathbf{r}) + \frac{1}{2} \left[\sum_{\alpha,\beta} (i\sigma_y)_{\alpha\beta} \Delta(\mathbf{r}) \psi_{\alpha}^{\dagger}(\mathbf{r}) \psi_{\beta}^{\dagger}(\mathbf{r}) + \text{h.c.} \right] + \sum_{\alpha,\beta} \psi_{\alpha}^{\dagger}(\mathbf{r}) (\mathbf{h} \cdot \boldsymbol{\sigma})_{\alpha\beta} \psi_{\beta}(\mathbf{r}) \Bigg\}. \tag{1}$$

The first term in brackets is the single-particle Hamiltonian for a quasiparticle with effective mass, m, Fermi energy, E_F, and scattering from a spin-independent potential $V_0(\mathbf{r})$. The pair potential, $\Delta(\mathbf{r})$, characterizes the spatial dependence to the superconducting singlet correlations, and will be calculated in a self-consistent fashion as described below. The ferromagnetic exchange field, $\mathbf{h}(y) = h_0 \hat{\mathbf{z}}$, representing the ferromagnetism, is taken as constant in the F layer and vanishing in the two S layers, and it is along the $\hat{\mathbf{z}}$ axis of quantization. This intrinsic exchange field in the magnet, favoring a given spin, thus contributes to the overall behavior of triplet correlations. The important spin-flip scattering will be assumed to be confined to the two interfaces near $y = d_S$ and $y = d_S + d_F$. It takes place in the invariant x-z plane: $\mathbf{V} \cdot \boldsymbol{\sigma} = V_x(y)\sigma_x + V_z(y)\sigma_z$. Its z component represents a less important local modification of the h_0 field, while V_x is the spin-flip term. We have taken $V_y = 0$ because of the geometry and also for convenience: including σ_y terms precludes the use of exclusively real numbers in the numerical diagonalizations and leads to additional technical irrelevant complications. Each of the triplet states can potentially exist over large length scales, thus allowing competing orderings to coexist.

To solve the problem we diagonalize $\mathcal{H}_{\text{eff}}$ via a Bogoliubov transformation. The details are given elsewhere[17] and need not be repeated here. Through the use of standard commutation relations, we end up after some straightforward algebra, a general coupled four component set of equations. This leads to a generalization of the textbook[26] Bogolioubov–de Gennes (BdG) equations, which give rise ultimately to spin singlet and triplet amplitudes. By making use of the Pauli spin matrices and of a set of Pauli-like matrices $\boldsymbol{\rho}$ in particle-hole space, the general time and spin-dependent BdG equations can be expressed compactly as

$$[\rho_z \otimes (\mathcal{H}_0 \hat{\mathbf{1}} - (h_z - V_z)\sigma_z) + (\Delta(y)\rho_x + V_x \hat{\mathbf{1}}) \otimes \sigma_x] \Phi_n(y,t) = i \frac{\partial \Phi_n(y,t)}{\partial t}, \tag{2}$$

where the four component wave function, $\Phi_n(y,t)$, is a vector of quasiparticle amplitudes, $\Phi_n(y,t) \equiv (u_{n\uparrow}(y), u_{n\downarrow}(y), v_{n\uparrow}(y), v_{n\downarrow}(y))^{\mathrm{T}} e^{-i\epsilon_n t}$, where the superindex denotes transposing, the $u_{n\sigma}$ and $v_{n\sigma}$ have their standard[26] meaning as quasiparticle amplitudes and ϵ_n is the eigenenergy. We have assumed here that E_F is the same throughout the sample: the majority (+) and minority (−) bandwidths in F are $E_F \pm h_0$.

The single-particle quasi-one-dimensional Hamiltonian $\mathcal{H}_0$ becomes in our geometry

$$\mathcal{H}_0 \equiv \frac{1}{2m}\frac{\partial^2}{\partial y^2} + \varepsilon_\perp - E_F + V_0(y), \tag{3}$$

where $\varepsilon_\perp$ is the energy in the transverse direction. Carrying the time derivative through, and taking the outer product in Eq. (2), we can rewrite Eq. (2) in the much less compact but intuitively more immediate form

$$\begin{bmatrix} \mathcal{H}_0 - h_z(y) + V_z(y) & V_x(y) & 0 & \Delta(y) \\ V_x(y) & \mathcal{H}_0 + h_z(y) - V_z(y) & \Delta(y) & 0 \\ 0 & \Delta(y) & -[\mathcal{H}_0 - h_z(y) + V_z(y)] & V_x(y) \\ \Delta(y) & 0 & V_x(y) & -[\mathcal{H}_0 + h_z(y) - V_z(y)] \end{bmatrix} \begin{bmatrix} u_{n\uparrow}(y) \\ u_{n\downarrow}(y) \\ v_{n\uparrow}(y) \\ v_{n\downarrow}(y) \end{bmatrix} = \epsilon_n \begin{bmatrix} u_{n\uparrow}(y) \\ u_{n\downarrow}(y) \\ v_{n\uparrow}(y) \\ v_{n\downarrow}(y) \end{bmatrix}, \tag{4}$$

where the spin-dependent interface scattering potential should be understood to be given in terms of delta function scatterers: $V_i(y) = V_i\{\delta(y-d_S) + \delta[y-(d_S+d_F)]\}$, and as explained above, $i=x,z$. The convenient dimensionless parameter $H_{spin} \equiv 2mV_x/k_F$ characterizes the strength of the interface scattering. The spin-flip x component, $V_x(y)$, technically complicates the calculation and prevents the simple splitting of the BdG equations into two separate equations by means of symmetry relations, as in the case of collinear magnetizations, or when a single quantization axis exists for the whole system. Here, all four components are needed since the exchange field in the ferromagnet as well as the spin-flip potential break the spin rotation invariance.

The general expression for the self-consistent pair potential, valid for all temperatures, T, is given by

$$\Delta(y) = \frac{g(y)}{2}\sum_n [u_n^\uparrow(y)v_n^\downarrow(y) + u_n^\downarrow(y)v_n^\uparrow(y)]\tanh\left(\frac{\epsilon_n}{2T}\right), \tag{5}$$

where the sum is over eigenstates [the index n now subsumes not only the quantized index in Eq. (4) but also the transverse energies $\varepsilon_\perp$] which is performed over all eigenstates with positive energies smaller than or equal to the "Debye" characteristic energy cutoff ω_D, and $g(y)$ is the superconducting coupling parameter that is a constant g_0 in the intrinsically superconducting regions and zero elsewhere.

The triplet correlation functions, odd in time, which are the main subject of our study are defined[17] in terms of the usual field operators as

$$f_0(\mathbf{r},t) \equiv \frac{1}{2}[\langle \psi_\uparrow(\mathbf{r},t)\psi_\downarrow(\mathbf{r},0)\rangle + \langle \psi_\downarrow(\mathbf{r},t)\psi_\uparrow(\mathbf{r},0)\rangle] \tag{6a}$$

$$f_1(\mathbf{r},t) \equiv \frac{1}{2}[\langle \psi_\uparrow(\mathbf{r},t)\psi_\uparrow(\mathbf{r},0)\rangle - \langle \psi_\downarrow(\mathbf{r},t)\psi_\downarrow(\mathbf{r},0)\rangle], \tag{6b}$$

where we are clearly free to choose one time coordinate to be zero, without loss of generality. These correlation functions must be odd in time because of the Pauli principle. Hence they vanish identically at $t=0$. At $T=0$, these expressions are conveniently written in terms of the quasiparticle amplitudes,[24]

$$f_0(y,t) = \frac{1}{2}\sum_n [u_{n\uparrow}(y)v_{n\downarrow}(y) - u_{n\downarrow}(y)v_{n\uparrow}(y)]e^{-i\epsilon_n t}, \tag{7a}$$

$$f_1(y,t) = \frac{1}{2}\sum_n [u_{n\uparrow}(y)v_{n\uparrow}(y) + u_{n\downarrow}(y)v_{n\downarrow}(y)]e^{-i\epsilon_n t}, \tag{7b}$$

where *all* positive energy states are in general summed over. For equal-time correlations, $t=0$, the above expressions vanish identically, in accordance with the Paul principle and follow mathematically via the four component quasiparticle completeness relations.[27] In practice, we find that at finite times, results become cutoff independent beyond a value a few ω_D. However, to ensure the vanishing of the triplet components at $t=0$, it is necessary to sum over a much larger energy range.

Besides the pair potential and the triplet amplitudes, we can also determine various physically relevant single-particle quantities. One such important quantity is the local magnetization, which is a measure of the so-called inverse proximity effect, and can be particularly useful in characterizing the magnetizing effects in the superconductor as a result of the localized spin-flip interface scattering and intrinsic exchange field of the magnet. It can also serve as an effective self-consistent measure of the magnetization field in the half-metal. Recent magneto-optical Kerr effect measurements[28] of a superconductor/ferromagnet bilayer revealed that the superconductor became magnetized, illustrating the need to determine the spatial behavior of the magnetization fully. In the presence of spin-flip scattering, the local magnetic moment $\mathbf{m}$ will depend on the coordinate y (in our geometry) and, in the presence of the spin-flip term it will have in general both x and z components, $\mathbf{m}=(m_x,0,m_z)$. In terms of the quasiparticle amplitudes calculated from the self-consistent BdG equations we have

$$m_z(y) = -\mu_B\sum_n [v_{n\uparrow}^2(y) - v_{n\downarrow}^2(y)], \tag{8a}$$

$$m_x(y) = -2\mu_B\sum_n v_{n\uparrow}(y)v_{n\downarrow}(y), \tag{8b}$$

where μ_B is the Bohr magneton. The sums in Eq. (8) involve a sum over eigenstates, as in Eqs. (5), although the energies

ϵ_n do not now appear explicitly. A very useful tool in the study of these phenomena is experimental tunneling experiments, where spectroscopic information, measured ideally by an STM, can reveal the local DOS. Therefore we have computed here also the local DOS $N(y,\epsilon)$ as a function of y. We have $N(y,\epsilon) \equiv N_\uparrow(y,\epsilon) + N_\downarrow(y,\epsilon)$, where,

$$N_\sigma(y,\epsilon) = \sum_n [u_{n\sigma}^2(y)\delta(\epsilon - \epsilon_n) + v_{n\sigma}^2(y)\delta(\epsilon + \epsilon_n)], \quad \sigma = \uparrow,\downarrow. \tag{9}$$

To elucidate the stability of the different configurations we will need to evaluate the free energy, for which, as in Ref. 16, we will use the expression,[29]

$$\mathcal{F}(T) = -2T\sum_n \ln\left[2\cosh\left(\frac{\epsilon_n}{2T}\right)\right] + \frac{1}{d}\int_0^d \frac{\Delta^2(z)}{g(z)}dz. \tag{10}$$

In order to numerically solve the problem, we must re-express the equations in terms of matrix elements in an appropriate basis. These matrix elements are obtained via projection upon a orthonormal complete set, that inherently satisfies the boundary conditions of vanishing wave function at the outer edges of the trilayer structure. Thus we write $u_{n\alpha}(y) = \sqrt{2/d}\Sigma_{q=1}^N u_{nq}^\alpha \sin(q\pi y/d)$, $v_{n\alpha}(y) = \sqrt{2/d}\Sigma_{q=1}^N v_{nq}^\alpha \sin(q\pi y/d)$, with $\sigma = \uparrow,\downarrow$. Inserting these into Eq. (4), we have the general $4N \times 4N$ matrix consisting of a 4×4 array of block submatrices, each of rank N,

$$\begin{pmatrix} \mathcal{H}^+ & \mathcal{V}^x & 0 & \mathcal{D} \\ \mathcal{V}^x & \mathcal{H}^- & \mathcal{D} & 0 \\ 0 & \mathcal{D} & -\mathcal{H}^+ & \mathcal{V}^x \\ \mathcal{D} & 0 & \mathcal{V}^x & -\mathcal{H}^- \end{pmatrix} \Psi_n = \tilde{\epsilon}_n \Psi_n, \tag{11}$$

where we measure all energies in terms of E_F, so that $\tilde{\epsilon}_n \equiv \epsilon_n/E_F$, $Z_{Bz} \equiv mV_z/(k_F^2 d)$, and the vector Ψ_n is the transpose of $(u_{n1}^\uparrow, \ldots, u_{nN}^\uparrow, u_{n1}^\downarrow, \ldots, u_{nN}^\downarrow, v_{n1}^\uparrow, \ldots, v_{nN}^\uparrow, v_{n1}^\downarrow \ldots, v_{nN}^\downarrow)$. We find, after lengthy but elementary algebra the matrix elements,

$$\begin{aligned} \mathcal{H}_{ij}^\pm = & \left[\left(\frac{i\pi}{k_F d}\right)^2 + \frac{\varepsilon_\perp}{E_F} - 1 \mp I\left[\frac{d_F}{d} + K_{2i}^{(1)} - K_{2i}^{(2)}\right]\right. \\ & \left. \pm Z_{Bz}(U_i^{(1)}U_j^{(1)} + U_i^{(2)}U_j^{(2)})\right]\delta_{ij} \\ & \mp I[K_{i+j}^{(1)} - K_{i-j}^{(1)} + K_{i-j}^{(2)} - K_{i+j}^{(2)}] \\ & \pm Z_{Bz}(U_i^{(1)}U_j^{(1)} + U_i^{(2)}U_j^{(2)}), \end{aligned} \tag{12}$$

where $I \equiv h_0/E_F$ and $Z_{Bz} \equiv 2V_z/E_F d$. The important spin-flip component, off the main diagonal, giving rise to equal-spin triplet correlations is

$$\mathcal{V}_{ij}^x = Z_{Bx}[U_i^{(1)}U_j^{(1)} + U_i^{(2)}U_j^{(2)}], \tag{13}$$

where $U_q^{(1)} = \sin(q\pi d_S/d)$, $U_q^{(2)} = \sin[q\pi(d_F + d_S)/d]$, $K_q^{(1)} = U_q^{(1)}/(q\pi)$, $K_q^{(2)} = U_q^{(2)}/(q\pi)$, and Z_{Bx} which arises from the spin-flip scattering is $Z_{Bx} \equiv 2V_x/E_F d$. This is related to the parameter $H_{spin} = 2mV_x/k_F$ defined earlier to characterize the spin-flip scattering, by $H_{spin} = k_F d Z_{Bx}/2$. Without loss of generality we can take $V_z = V_x = V_{spin}$. The matrix elements corresponding to the pair potential are $\mathcal{D}_{ij} = 2/(E_F d)\int_0^d dy \Delta(y)\sin(i\pi y/d)\sin(j\pi y/d)$, recalling that $\Delta(y)$ vanishes in the magnet layer, due to the coupling $g(y)$. Since we are not permitted to use previous symmetry relations among the quasiparticle amplitudes and energies that reduced the matrix eigensystem to $2N$, we are forced, as mentioned above, to solving the $4N \times 4N$ system, and retaining only the positive energy states. As in previous work, the diagonalization is performed iteratively until the self-consistency condition Eq. (5) is satisfied.

III. RESULTS

The results of our calculations are described in detail in this section. We will measure all the lengths in units of the Fermi wave vector k_F, and define the relative dimensionless coordinate $Y \equiv k_F(y - d/2)$, i.e., $Y = 0$ is at the center of the junction. All times will be given in units of ω_D^{-1} via the dimensionless time $\tau \equiv \omega_D t$. In the ferromagnet we have for the spin up and spin down band widths, $E_\uparrow = E_F + h$ and $E_\downarrow = E_F - h$. The dimensionless measure of the intrinsic exchange energy in the magnet is $I \equiv h/E_F$. All results below are for the half-metallic limit, $I = 1$, discussed recently in the context of spintronic materials.[30] The spin-flip scattering at the interface is characterized, as previously explained, by the dimensionless parameter H_{spin} for which we will consider values between zero and unity. Geometrically, we will consider a system consisting of two thick superconducting layers, each of a thickness d_S such that $D_S \equiv k_F d_S = 300$. Since odd-frequency or different-time triplet states arise from magnetic effects at the interfaces and exchange field in the half-metal, this broad range of parameters will give revealing hints as to their existence. The chosen d_S considerably exceeds the superconducting coherence length ξ_0, which we take to be $\xi_0 = 50k_F^{-1}$. Thus $d_S = 6\xi_0$, so that we can disentangle quantum interference effects from the modified Andreev and scattering events at a spin-flip interface. The two S layers are separated by a ferromagnetic layer, which must be taken to be thin enough so that the two superconductors are still coupled through the F material via the proximity effect. We take $D_F \equiv k_F d_F = 10$. All results are computed in the low temperature limit.

Each junction between two consecutive S layers can be of the "0" type (with the order parameter in both S layers having the same sign) or of the "π" type (opposite sign). The characteristics of a 0 or π junction are directly connected to the spatial behavior of the pair potential $\Delta(y)$ and, to determine its precise form, this quantity must be calculated self-consistently so that the resulting singlet pair amplitude corresponds to a minimum in the free energy. The relative stability of the different states that may be obtained through self-consistent solution of the BdG equations depends on the free energy of the junctions. We therefore consider first the stability of the system for our parameter values and geometry. In Fig. 1 we plot the condensation energy [the free energy as given in Eq. (10) at $T = 0$] of the system in dimensionless form, that is, in units of $N(0)\Delta_0$ where $N(0)$ is the usual single spin density of states in the S material, and Δ_0 the bulk value of the gap. Thus, the quantity plotted would be $-1/2$ for a bulk S sample. This energy is calculated with

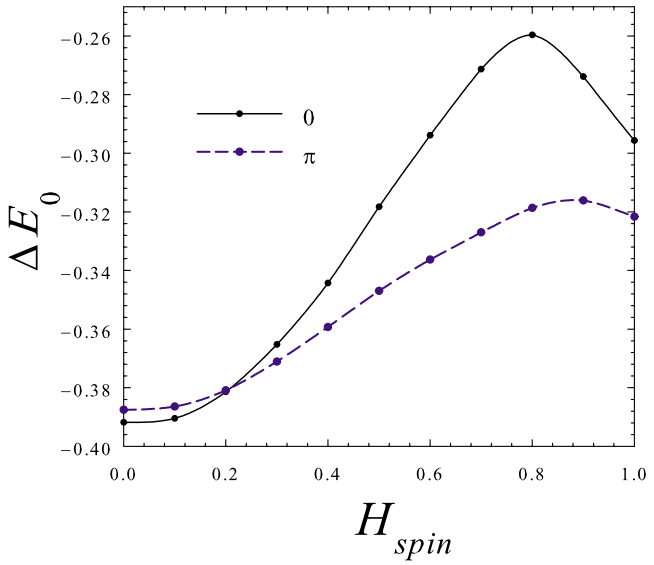

FIG. 1. (Color online) The dimensionless condensation energy [free energy at $T=0$ in units of $N(0)\Delta_0$, see text], versus the dimensionless parameter H_{spin} characterizing the spin-flip strength at the interface, for an SFS junction with a half-metallic ferromagnet. For the geometry chosen, we see that the both the π and the 0 states are stable for all values of H_{spin} considered and that the π state has the lower condensation energy except at small values of H_{spin}.

high precision as explained in previous[16] work. We see in the figure that, consistent with the results of Ref. 16, the condensation energies are reduced, in all cases, from what they would be for a bulk S sample. For all values of H_{spin} both the 0 and π configurations of the structure are at least locally stable, but in general nondegenerate, showing that indeed the two S slabs are indeed coupled via the proximity effect. At very small values of the spin-flip parameter, the 0 configuration is the stable one, but this changes as H_{spin} increases: there is a first-order phase transition at $H_{spin} \lesssim 0.2$ and at larger values of H_{spin} the π configuration is the stable one and the 0 configuration is much less stable. The 0 configuration metastable minimum is shallowest at $H_{spin} \approx 0.8$ where the condensation free energy has a sharp maximum. The condensation free energy of the π state is more weakly dependent on H_{spin} with a maximum near $H_{spin}=0.82$ much shallower than that found in the 0 state. Note that by decreasing the width of S, the qualitative results remain, but the overall results are shifted toward zero, resulting in the possible elimination of the zero state altogether. In general, computational convergence time is increased as the condensation for a given state approaches zero.

We turn next to the spatial dependence of the general complex triplet pairing functions $f_0(Y,\tau)$ and $f_1(Y,\tau)$ as defined in Eqs. (7). In Fig. 2 we plot the corresponding triplet amplitudes for each of the two types of solution (0 or π) as a function of the dimensionless coordinate Y and at fixed time, $\tau=20$, for six equally spaced values of H_{spin} in the range $0 \leq H_{spin} \leq 1$ (see legends). All amplitudes plotted are normalized to Δ_0/g, so that, if the similarly normalized ordinary singlet amplitude were plotted, it would reach unity deep in bulk S material. The value $\tau=20$ is chosen as being near[16] that which maximizes the correlations, and is such that the triplet pairing states have penetrated most of the two superconductor regions. Results for the first group of four plots are for the 0-state solutions, and with the real and imaginary triplet amplitudes labeled accordingly. The bottom series of four panels are for the π junction counterparts. The range of Y included in the plots is, for clarity, somewhat narrower than the sample size: regions where the amplitudes are very small or zero are omitted. One can see that the amplitude f_1 vanishes identically in the absence of spin-flip scattering, since in that case both the total spin and its z component are good quantum numbers. For finite values of the spin-flip parameter, all possible projections of the total spin exist. The spatial symmetry of the singlet Cooper pair is also reflected in the triplet pairing states: it is evident from this and the next figure that if the singlet order parameter is in a 0 junction state, the corresponding triplet amplitudes maintain that symmetry. This holds true for the spatially antisymmetric π junction results as well (bottom four panels).

Turning our attention to the real part of f_1 for the 0 state we see that it shows a monotonic decline in magnitude from the interface, over about three to four coherence lengths, for the largest two spin-flip strengths (with a superposition of rapid oscillations). The remaining weaker scattering strengths are quite different in that they yield nonmonotonic behavior with a maximum deep into S at about $2\xi_0$, and then decaying to zero at roughly $4\xi_0$ (hence for $H_{spin}=0.8$, this correlation dies about ξ_0 earlier). These amplitudes, Re f_1, are predominately positive for higher spin transparency (smaller H_{spin}) junctions, and then undergo a sign flip for the stronger H_{spin}. If we examine now the imaginary component Im f_1, still for the 0 state, we see similar opposite parity effects separating the strongest H_{spin} from the weaker values, here however there is a clearer separation between the curves. The time dependence here is noticeably different than for the real part; the triplet correlations have a faster rate of propagation, in that they have reached deeper within the sample for the same τ. We have emphasized the triplet amplitudes in the S region, however these plots reveal that besides the expected fact that $\langle \psi_\uparrow(y,t)\psi_\uparrow(y,0)\rangle$ is not destroyed by the half-metal, by including the proximity effects in a self consistent way, we found non-negligible different spin triplet pairing in the half-metal, but with a smaller magnitude that f_1.

The π state results for the equal-spin pairing correlations have markedly different profiles than those for the 0 state: besides being highly peaked at the interface, where spin-flip scattering originates, Re f_1 has a very weak dependence on H_{spin}, with an abrupt emergence only for the highest H_{spin} and then still decaying over roughly the same distance in S. Overall, the π state f_1 amplitudes are suppressed, even for the case when both the 0 and π states have the same condensation energy ($H_{spin} \approx 0.2$). The diminished π state results arises partly from the symmetry requirements imposed upon f_i: $f_i(-Y)=-f_i(Y)$, thus in F, the f_i amplitudes vanish at $Y=0$, which can constrain the overall longer range spatial behavior. It can be concluded that the singlet Cooper pair order parameter that minimizes the free energy, and which $|\Delta(Y)|$ is typically larger, does not necessarily result in the larger triplet amplitudes. The imaginary parts can be discerned from the figure, but clearly the imaginary parts to the

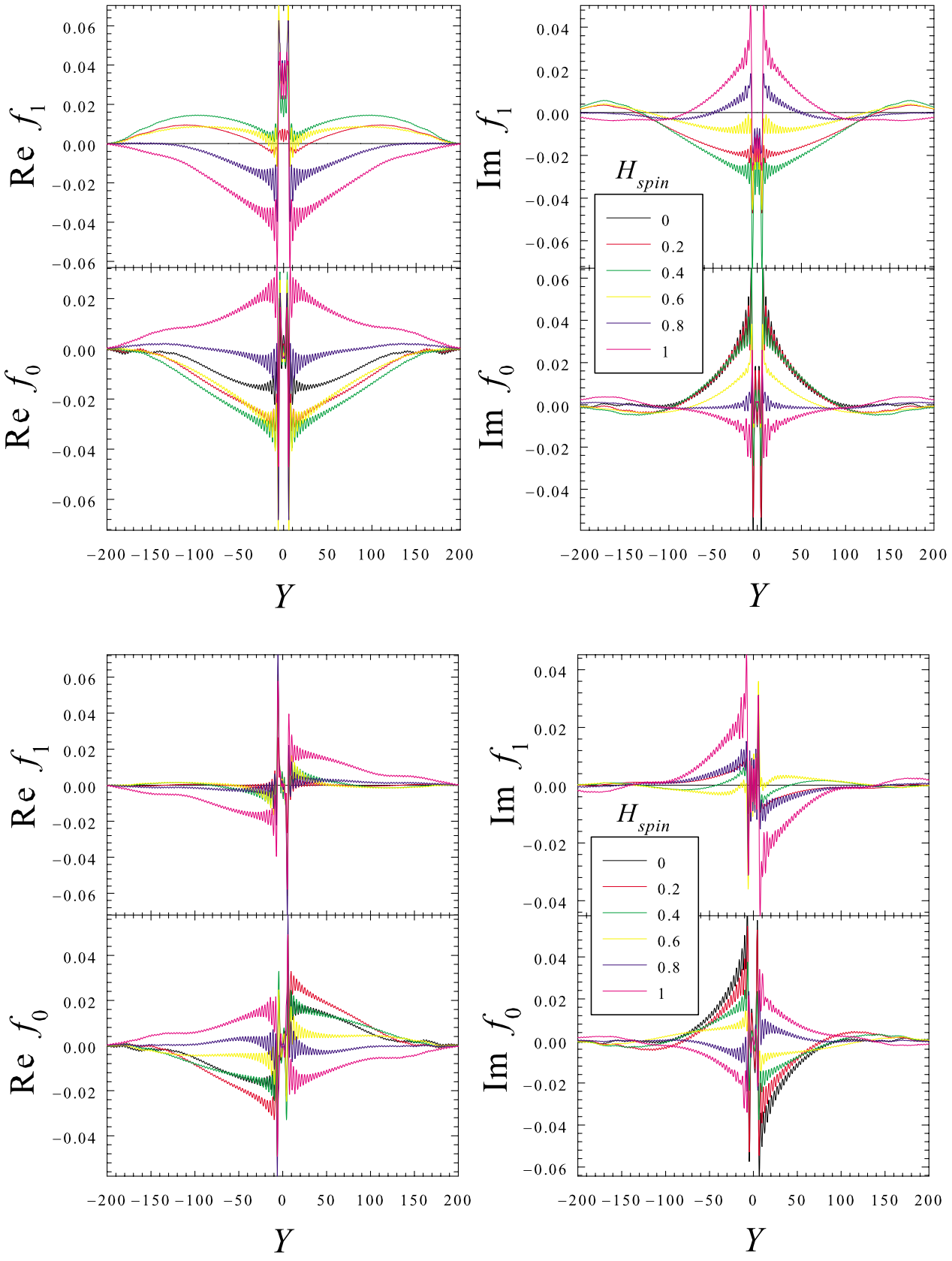

FIG. 2. (Color online) The f_1 and f_0 triplet pair amplitudes [Eq. (7)] for a 0 junction (top four panels) and π junction (bottom four panels) plotted as a function of the dimensionless coordinate Y for several values of H_{spin} as indicated in the legend. The left panels show the real parts while the right ones show the imaginary parts, for values of H_{spin} ranging from 0 to 1. All results are at a fixed value of the dimensionless time, $\tau=20$.

amplitudes also do not simply differ by a phase. Also, some amplitudes oscillate (with periods on the order of ξ_0) while other plots show simple declines, with atomic scale oscillations superimposed on the general profile.

The $m=0$ triplet amplitude, f_0, with zero projection of the z component of total spin, does not vanish, at any finite time, even for $H_{spin}=0$ since the total spin (as opposed to its z component) is not a good quantum number in the presence of the F material. It does still vanish at $t=0$ because of the Pauli principle. Thus, in general, when a single quantization axis exists for the system, f_0 coexists with the ordinary singlet s-wave component. We expect the results for f_0 to be different those for f_1 since f_0 does not emerge solely from H_{spin}: there are two competing spin-flip effects in the z direction: the magnetization of the half-metal, and the spin-dependent scattering at the interface. It is clear from the form of the BdG Eq. (4) that these two effects compete against each other. For both the 0 and π state, the absolute value of a given component of f_0 at fixed time in S is again a nonmonotonic function of H_{spin}, but the overall dependence is visibly different. The maximum value of f_0 in S is always at the interface: this is as expected from the above considerations regarding quantum numbers. The behavior with H_{spin} echoes (at larger values) that found for f_1, and for the same reasons. In all cases, these triplet correlations clearly pervade the thin F layer, while their penetration into S increases only weakly with H_{spin}.

In Fig. 3 we show results for the triplet amplitudes in the same format as in Fig. 2 but at fixed H_{spin} and several values of τ, so that the explicit time evolution of the different-time triplet states can be visualized. As before, the real or imaginary part of f_0 or f_1 is appropriately labeled whether discussing the 0 or π state configurations (top four or bottom four panels, respectively). All results are for an intermediate spin-flip transparency $H_{spin}=0.2$, where both junction states have very approximately the same condensation energy (see Fig. 1). The region of the sample shown here is wider than that in Fig. 2 because the spatial range over which the correlations extend is now wider, at larger times. We see than the triplet correlations, which of course vanish identically at $\tau=0$ already pervade the S layer at the earliest times shown. The real part of the amplitude f_1 has, in the 0 state, a maximum in the S region that keeps propagating outward as τ increases, reflecting the longer penetration of the correlations into S. This maximum becomes shallower with increasing τ however. This increased penetration occurs also for both the real and imaginary components of f_0, although in the latter case the maximum value of the amplitude in S occurs near the interface except in some instances at the longest times studied. The largest τ studied was determined by the need to avoid finite size effects: after the different-time correlations have pervaded the entire S portion of the sample the results would be contaminated by outer boundary effects. Referring still to the 0 state, we again have the situation where for a given time τ and fixed value of H_{spin}, the Im f_1 tends to have pervaded more of the superconductor region than the real part. The π amplitudes have some similarities with those in Fig. 2, in that Re f_1 is smaller and has a weak dependence on the scattering strength. Although Im f_1 demonstrates a stronger dependence on H_{spin}, and besides prominently peaking at the interfaces, the overall magnitudes for both components are effectively reduced for all values of τ shown.

This penetration of the triplet correlations into the S material can be conveniently described in terms of time-dependent penetration depths. These can be calculated for either f_0 or f_1. We will focus here on the real parts of f_1, with the understanding that an analogous approach could be followed for either f_0 or the imaginary components. However, it is also evident from Fig. 2 that for f_0, the penetration of triplet correlations into S is only weakly dependent on H_{spin}, which is consistent with the fact that f_0 does not emerge from H_{spin} only. The method to extract any sort of characteristic length depends of course on the problem at hand, and for the f_1 amplitudes we find the following definition yields sensible results,

$$\ell(\tau) = \frac{\int_S dY |Y - Y_0| |\mathrm{Re}\{f_1(Y,\tau)\}|}{\int_S dY |\mathrm{Re}\{f_1(Y,\tau)\}|}, \tag{14}$$

which is slightly modified from that used previously.[17] The definition Eq. (14) accounts better for cases where the overall shape of the amplitudes (see Figs. 2 and 3) varies depending on the parameter values. The coordinate shift, $Y-Y_0$, accounts for measuring the distance from the interface: for our coordinates, $Y_0=D_F/2$ and the integration extends over the S region. This definition gives the expected result if the function f_1 were a pure decaying exponential. The values of the dimensionless ℓ are in units of k_F^{-1}. The results are plotted in Fig. 4 as a function of τ. These results are for the same range of H_{spin} as in the previous figures, as shown in the legend. Both the 0 (top) and π (bottom) state penetration depths are shown. There is an approximately linear behavior, in both 0 and π cases, at earlier times and a deviation from linearity at later times. For the 0 state, the values of ℓ reach discernible maxima that get shifted to larger times with increased spin-dependent scattering rates. For larger values of H_{spin}, the times necessary to reach the peak would presumably correspond to times where these triplet correlations would have reached the boundary and finite size effects would be a concern. This increase for larger H_{spin} should not continue beyond a characteristic time,[17] after which the triplet correlations would saturate. It is clear, however, that the penetration extends over a wide range of times over regions much larger than the superconducting coherence length. The results here are consistent with what we saw in Fig. 2, where at $\tau=20$, we see for $H_{spin}=0.2$, 0.4, and 0.6, the manifestation of secondary broad maxima at large Y, and little variation among the f_1 amplitudes, while the other values (0.8 and 1) have generally a monotonic decline, and thus for these higher values they have smaller characteristic penetration depths. The penetration of equal-spin triplet correlations into a π junction is much less dependent on the spin scattering strength than for 0 junctions except of course at very small H_{spin}. This is again consistent with what was shown in Fig. 2, where the real parts of the f_1 correlations demonstrated very little dependence on H_{spin}, and were weaker overall, away from the interface, than their 0 junction counterparts. This is reflected in the penetration depth behavior, where the depth is reduced compared to the π case and the penetration is similar for the

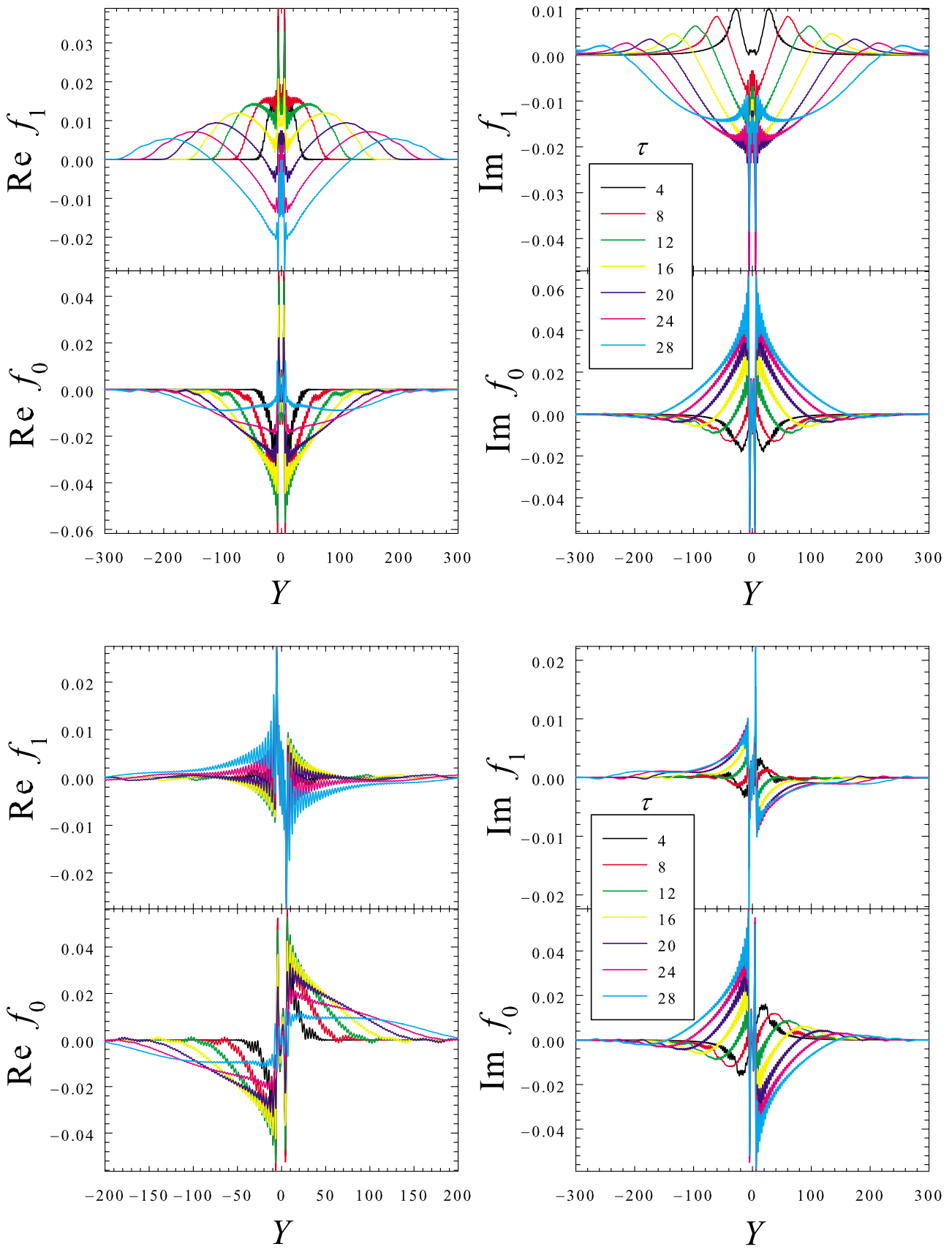

FIG. 3. (Color online) The temporal dependence of the 0 and π state junction triplet amplitudes. They are arranged as in Fig. 2 and plotted as a function of Y for several equally spaced values of τ. These results are at a fixed value of the spin-flip parameter, H_{spin}=0.2, where both the π state and the 0 state are stable (see Fig. 1).

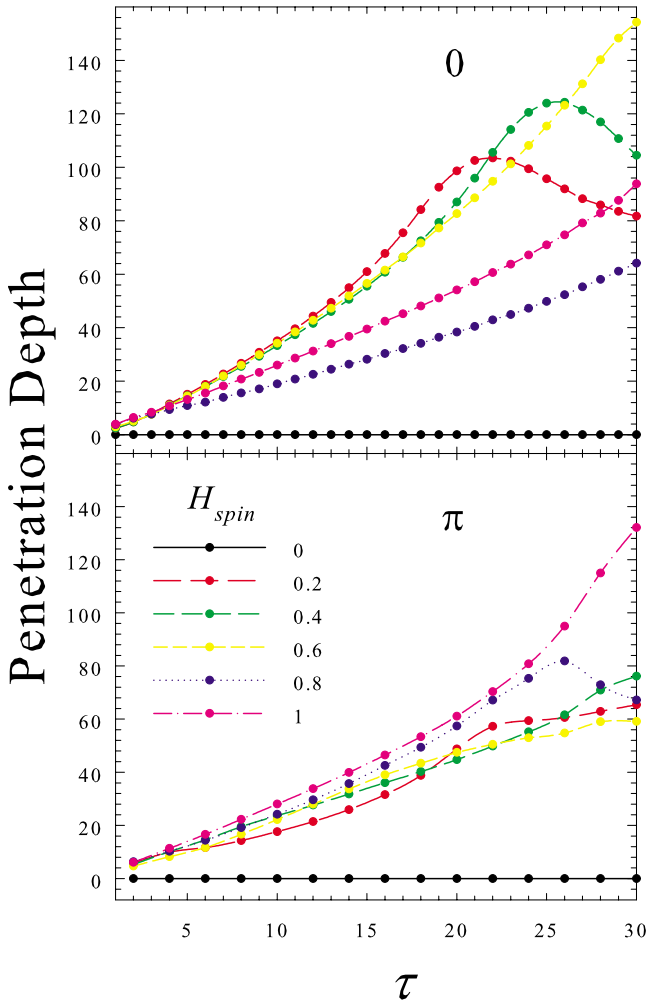

FIG. 4. (Color online) The penetration depth, as defined in dimensionless units in Eq. (14), of the equal-spin f_1 triplet component into the S material, plotted as a function of τ for both the "0" and "π" configurations (as labeled).

broad range of spin-dependent scattering strength. The only exception being the extreme case of $H_{spin}=1$, which always has a greater penetration, but this too agrees well with what is observed in Fig. 2.

The density of states, measured in principle by in STM experiments, is one way of probing indirect evidence of the triplet superconducting states, and carries valuable energy-resolved spectroscopic information. We therefore show next, in Fig. 5, the DOS, computed from Eq. (9). For computational purposes, we represent the delta functions in Eq. (9) as the low T limit of the derivative of the corresponding Fermi functions. We find that a fine mesh of $\varepsilon_\perp$ is necessary to properly calculate the energy-resolved DOS, and that there are significant contributions to the DOS from both longitudinal propagation (small $\varepsilon_\perp$) and from large off-normal incidence at the interface (large $\varepsilon_\perp$). The junction here is therefore not appropriately described within the tunneling limit,[31] and would yield differing results if only a narrow tunneling cone was used in the calculation. By considering spin-active interfaces, it was shown[32] that various signatures arise in the DOS, including a unique double gap structure. In Fig. 5 the DOS is shown, normalized to its bulk value in S, as a function of energy ϵ (relative to E_F), in units of the bulk Δ_0. We consider four values of H_{spin} for both the 0 state (left panels) and the π state (right panels). The top panels shows results summed over both spins and averaged over the entire thin F layer (label "F") while the bottom panels shows results (also summed over spins) averaged over the whole length of one of the superconductors (label "S"). For the S regions, in both the 0 and π junctions there are BCS-type peaks at $\epsilon/\Delta_0 \approx \pm 1$, reflecting the bulklike behavior. Inside the region of the bulk gap there is a secondary structure reflecting Andreev states. These secondary peaks were also found in Ref. 33. We also see that the subgap peaks arise even in the absence of interface spin activity (at $|\epsilon/\Delta_0| \approx 0.5$), and originate mainly from individual spin channels, depending on the sign of the energy: the prominent subgap peak at negative energy is due to the occupation of spin-up quasiparticles, $N_\uparrow$, while its positive energy counterpart arises from $N_\downarrow$. The position of these subgap peaks varies with H_{spin} in a way that seems to reflect the condensation energy in Fig. 1, particularly in the 0 state. At higher energies, $|\epsilon/\Delta_0| > 1$, both spin bands contribute equally to the DOS. In general within S and for the range of energies shown, the approximate relation, $N_\uparrow(\epsilon) \approx N_\downarrow(-\epsilon)$, holds, giving the observed symmetry in energy for the total DOS in the S region (Fig. 5 bottom panels). Increasing H_{spin}, tends to flip the spins at the interface, and thus bound states in S predominantly occupied by a given spin species, become replaced by the opposite spin quasiparticles. This is confirmed by examination of the individual spin density of states [Eq. (9)]. The half-metallic ferromagnet modifies this bound state picture in that region due to the existence of only one spin band at the Fermi level (top panels). Here the majority of the energy-resolved states must come from spin-up quasiparticles. The spin-flip processes inherent to the scattering events at the interface (the parameters H_{spin} or I) in conjunction with proximity effects can however cause an enhancement of subgap bound states at small energies attributed to a small number of minority spin states in the magnet. Also due to the strong spin splitting in that region, there is significant particle-hole asymmetry. At higher values of $|\epsilon/\Delta_0|$ the correct limit is approached $[\approx (1/2)(1+I)^{1/2}]$. The structure in the region $|\epsilon/\Delta_0| < 1$ is now considerably more complicated but consistent with what is seen in the S region: the number of states at zero energy is greater when the condensation energy is very small (see Fig. 1). We turn now to the trends the peaks in S follow as a function of H_{spin}, for both junction configurations. As H_{spin} is increased from 0 to about 0.8, the value at which the condensation free energies are near their minimum values (see Fig. 1), we see that these peaks tend to merge and there is a zero-energy single or double peak signature, depending on whether it is a π or 0 junction respectively. For $H_{spin}=1$, the peaks widen, to nearly the same energies as for $H_{spin}=0.4$. It does appear that for both junction states, depending on the spin strengths, there exists a small subgap region which resembles an energy gap in the DOS. Strictly speaking, however, the energy spectrum is gapless for the whole range from no spin flipping to strong activity at the interface; there is always a finite, albeit small in some cases, number of states within this Andreev bound state region. Adding a sufficiently strong spin-

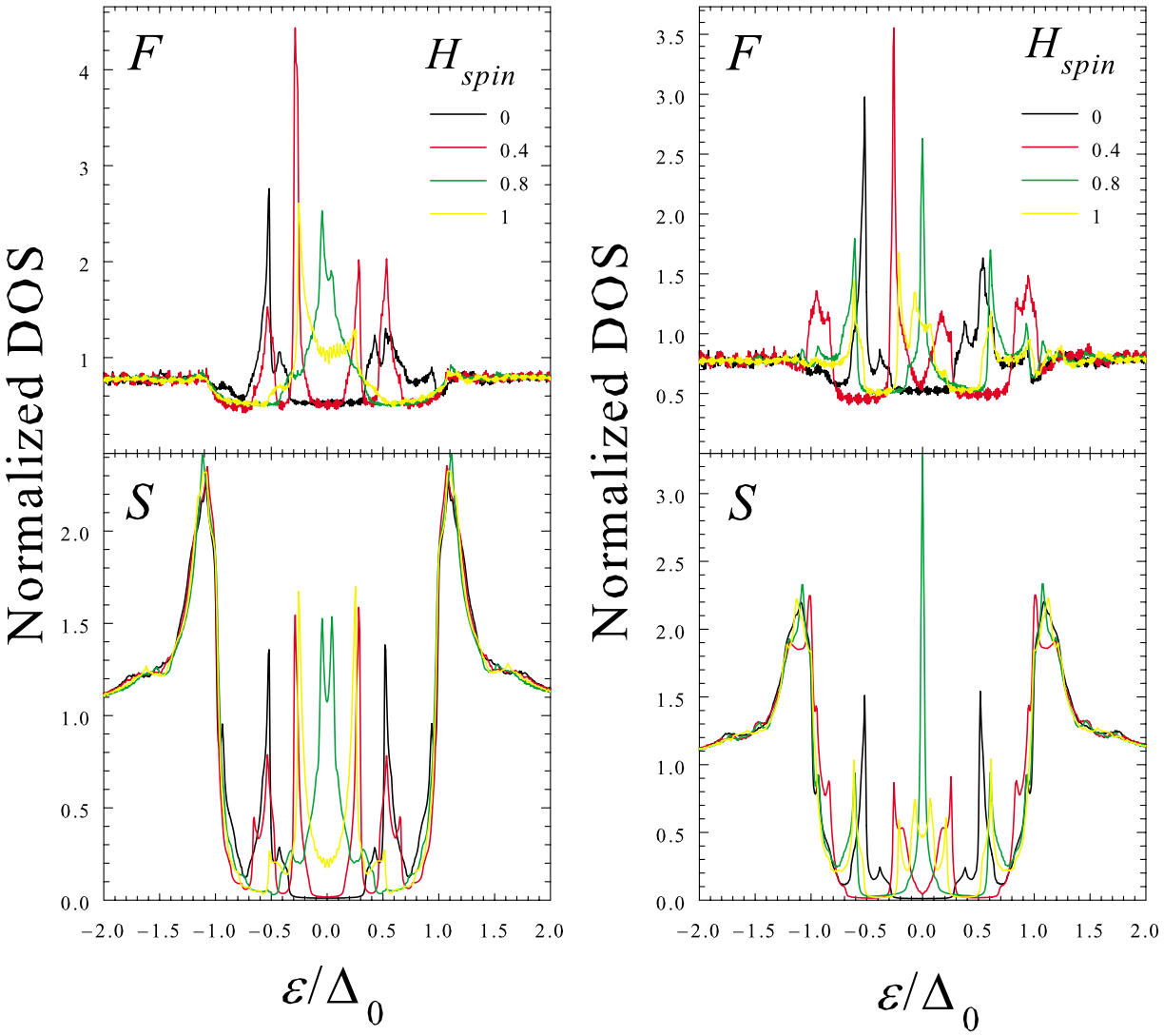

FIG. 5. (Color online) The local density of states, normalized to unity in the normal state of the S material. The top panels show results within the thin F layer, while the bottom one is for the superconductor. The left column is for the 0 state and the right one for the π state.

independent scattering or further increasing d_S would eventually create a region with no states. The existence of the half-metal and the interface scattering thus still influences the superconductor when considering spatially averaged behavior.

To gain further insight into the relative proximity effects inherent to these junctions, we present in Fig. 6 results for the influence of H_{spin} on the inverse proximity effect, that is, on the local magnetic moment as defined in Eq. (8). We find that if the large $\varepsilon_\perp$ off-normal trajectories are not fully included, the magnetic moment does not reach its proper normalized values and spatial properties. The calculation of m_z and m_x thus serves as another check to ensure that all the requisite states are included for other calculations. The results for the local magnetization [as defined above in Eq. (8) and normalized by μ_B] are shown in Fig. 6. They display the penetration of the magnetization into the superconductor region, as well as the weakening spin polarization in F. This is currently a topic of extreme interest, experimentally and theoretically, especially when trying to clarify the complicated spin structure in these systems. One can also view the introduction of spin scattering as an ultra narrow domain wall at the interfaces. In the figure both the x and the z components of the local magnetic moment are plotted as a function of Y for several values of H_{spin} in the range $0 \leq H_{spin} \leq 1$. The results are the same for 0 and π states. Results for the 0 state are shown. The x component vanishes by symmetry since the exchange field lies in the z direction when $H_{spin}=0$. At nonzero values of this parameter, m_x grows very quickly in the interface region, while remaining zero in the center of the F layer and also, of course, deep in the superconductor. For this reason only the central part of the system is included in the plot. The z component (bottom panel) has a very weak variation with H_{spin} near the center, $Y=0$, of the half-metal, but it does show a dependence on the scattering strength in the superconductor near the interface. The inverse proximity effect is clearly evident where the induced magnetization component m_z in the S region near the interface is oppositely directed to that in F, effectively screening the magnetization in F, by an amount that increases

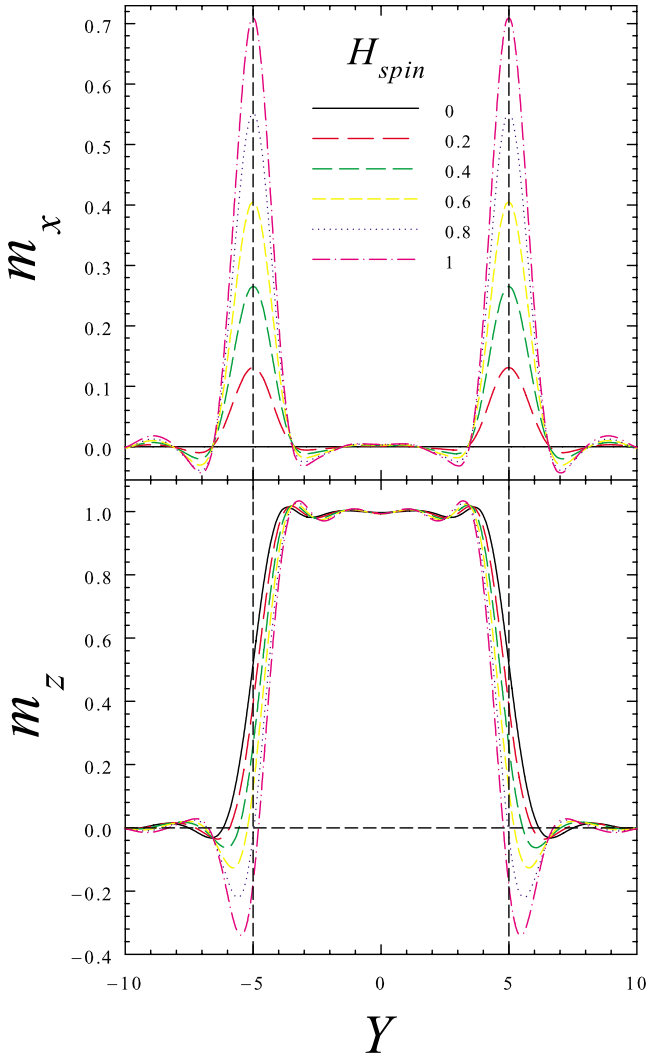

FIG. 6. (Color online) The x (top panel) and z components (bottom panel) of the local magnetic moment normalized by μ_B [see Eq. (8)] plotted as a function of the dimensionless coordinate Y for H_{spin}=from 0 to 1 at 0.2 intervals. Only a limited range of Y is included. The 0 and π state results are identical for the entire range of spin flipping considered here.

monotonically with H_{spin}. On the ferromagnet side very near the interface, this component of the magnetic moment correspondingly weakens with increased H_{spin}, before rising up to near the half-metallic bulk value of unity. The screening effect in the superconductor is apparently stronger for m_z than m_x. For the latter the induced magnetic moment is very similar in adjacent regions near the boundaries, and there is near symmetry about the interfaces. The component m_x reverses signs in both F and S for all H_{spin}, while m_z is briefly negative for only the larger H_{spin}, demonstrating the competing effects from the exchange field and spin scattering strength. The observed spatial characteristic of each component in Fig. 6 reveal that **m** in the vicinity of the interfaces tends to not only change magnitude as a function of position, but it also *rotates*. The magnetization also changes direction as a function of H_{spin} for fixed Y, illustrating again the important role the proximity effects play on the relevant self-consistent quasiparticle wave functions and energies.

IV. CONCLUSIONS

We have investigated the effect of interfacial spin-flip scattering on the triplet correlations that emerge in an SFS trilayer. We have studied this system by solving in a fully self-consistent way the BdG equations in the clean limit. We have considered both 0 and π junctions and found that the results depend strongly on the junction state. Triplet amplitudes, odd in time as required by the Pauli principle, have been found to exist and we have studied them in detail for the case where F is half-metallic. We have found that the $m=\pm 1$ triplet amplitudes emerge and then subsequently increase (at finite times) very rapidly with the dimensionless spin-flip parameter H_{spin}. The degree at which the equal-spin triplet correlations pervade the S layers has been discussed in connection with the respective penetration depths. We also have presented results for the local energy-resolved DOS averaged over both the S and F regions as a function of the spin-flip rate. The 0 or π state signatures may provide clues as to how different-time triplet states indirectly influence the subgap energy spectrum. We have also considered the inverse proximity effect (the penetration of the magnetization into S and its weakening in F) and found that near the interfaces the magnetization rotates as a function of position or of H_{spin}. Ultimately, the induced spin imbalance in the superconductor effectively screens the polarizing effects of the half-metal.

ACKNOWLEDGMENTS

This project was supported in part by a grant of supercomputer resources provided by the DoD High Performance Computing Modernization Program (HPCMP) and NAVAIR's ILIR program sponsored by ONR. We thank I. Krivorotov for useful discussions.

*klaus.halterman@navy.mil
†Also at Minnesota Supercomputer Institute, University of Minnesota, Minneapolis, Minnesota 55455; otvalls@umn.edu

[1] A. I. Buzdin, Rev. Mod. Phys. **77**, 935 (2005).
[2] I. Žutić, J. Fabian, and S. Das Sarma, Rev. Mod. Phys. **76**, 323 (2004).
[3] V. L. Berezinski, JETP Lett. **20**, 287 (1974).
[4] F. S. Bergeret, A. F. Volkov, and K. B. Efetov, Phys. Rev. Lett. **86**, 4096 (2001).
[5] F. S. Bergeret, A. F. Volkov, and K. B. Efetov, Rev. Mod. Phys. **77**, 1321 (2005).
[6] R. S. Keizer *et al.*, Nature (London) **439**, 825 (2006).
[7] M. Cuoco, W. Saldarriaga, A. Polcari, A. Guarino, O. Moran, E. Baca, A. Vecchione, and P. Romano, Phys. Rev. B **79**, 014523

(2009).
[8] M. van Zalk, M. Veldhorst, A. Brinkman, J. Aarts, and H. Hilgenkamp, Phys. Rev. B **79**, 134509 (2009).
[9] T. Kubota, S. Tsunegi, M. Oogane, S. Mizukami, T. Miyazaki, H. Naganuma, and Y. Ando, Appl. Phys. Lett. **94**, 122504 (2009).
[10] M. Vélez, M. C. Cyrille, S. Kim, J. L. Vicent, and I. K. Schuller, Phys. Rev. B **59**, 14659 (1999).
[11] V. N. Krivoruchko and V. Yu. Tarenkov, Phys. Rev. B **75**, 214508 (2007).
[12] P. SanGiorgio, S. Reymond, M. R. Beasley, J. H. Kwon, and K. Char, Phys. Rev. Lett. **100**, 237002 (2008).
[13] M. Eschrig, J. Kopu, J. C. Cuevas, and G. Schön, Phys. Rev. Lett. **90**, 137003 (2003).
[14] M. Eschrig and T. Löfwander, Nat. Phys. **4**, 138 (2008).
[15] J. Linder, M. Zareyan, and A. Sudbo, Phys. Rev. B **79**, 064514 (2009).
[16] P. H. Barsic, O. T. Valls, and K. Halterman, Phys. Rev. B **75**, 104502 (2007).
[17] K. Halterman, O. T. Valls, and P. H. Barsic, Phys. Rev. B **77**, 174511 (2008).
[18] J. Linder, T. Yokoyama, and A. Sudbø, Phys. Rev. B **77**, 174514 (2008).
[19] Y. V. Fominov, A. F. Volkov, and K. B. Efetov, Phys. Rev. B **75**, 104509 (2007).
[20] Y. Asano, Y. Tanaka, and A. A. Golubov, Phys. Rev. Lett. **98**, 107002 (2007).
[21] G. B. Halasz, J. W. A. Robinson, J. F. Annett, and M. G. Blamire, Phys. Rev. B **79**, 224505 (2009).
[22] M. Fauré, A. I. Buzdin, A. A. Golubov, and M. Yu. Kupriyanov, Phys. Rev. B **73**, 064505 (2006).
[23] S. Takahashi, S. Hikino, M. Mori, J. Martinek, and S. Maekawa, Phys. Rev. Lett. **99**, 057003 (2007).
[24] K. Halterman, P. H. Barsic, and O. T. Valls, Phys. Rev. Lett. **99**, 127002 (2007).
[25] K. Halterman and O. T. Valls, Phys. Rev. B **70**, 104516 (2004).
[26] P. G. deGennes, *Superconductivity in Metals and Alloys* (Addison-Wesley, Reading, MA, 1989).
[27] J. B. Ketterson and S. N. Song, *Superconductivity* (Cambridge University Press, Cambridge, England, 1999).
[28] J. Xia, V. Shelukhin, M. Karpovski, A. Kapitulnik, and A. Palevski, Phys. Rev. Lett. **102**, 087004 (2009).
[29] I. Kosztin, Š. Kos, M. Stone, and A. J. Leggett, Phys. Rev. B **58**, 9365 (1998).
[30] M. I. Katsnelson, V. Yu. Irkhin, L. Chioncel, A. I. Lichtenstein, and R. A. de Groot, Rev. Mod. Phys. **80**, 315 (2008).
[31] J. Linder, T. Yokoyama, A. Sudbo, and M. Eschrig, Phys. Rev. Lett. **102**, 107008 (2009).
[32] A. Cottet and J. Linder, Phys. Rev. B **79**, 054518 (2009).
[33] K. Halterman and O. T. Valls, Phys. Rev. B **69**, 014517 (2004).